

## Silicon doping dependence of highly conductive $n$ -type $\text{Al}_{0.7}\text{Ga}_{0.3}\text{N}$

K. Zhu, M. L. Nakarmi, K. H. Kim, J. Y. Lin, and H. X. Jiang<sup>a)</sup>  
*Department of Physics, Kansas State University, Manhattan, Kansas 66506-2601*

(Received 7 January 2004; accepted 21 September 2004)

Highly conductive Si-doped  $n$ -type  $\text{Al}_{0.7}\text{Ga}_{0.3}\text{N}$  alloys were grown by metalorganic chemical vapor deposition on sapphire substrates. Variable temperature Hall-effect measurements have been employed to study the electrical properties for samples with nominal Si dopant concentration ( $N_{\text{Si}}$ ) from  $2.6$  to  $6.8 \times 10^{19} \text{ cm}^{-3}$ . For the sample with  $N_{\text{Si}} = 6.0 \times 10^{19} \text{ cm}^{-3}$ , we have achieved  $n$ -type resistivity of  $0.0075 \Omega \text{ cm}$  with an electron concentration of  $3.3 \times 10^{19} \text{ cm}^{-3}$  and mobility of  $25 \text{ cm}^2/\text{V s}$  at room temperature. For the same sample, the effective donor (Si) activation energy  $E_0$  was determined to be as low as  $10 \text{ meV}$ .  $E_0$  increases to  $25 \text{ meV}$  as  $N_{\text{Si}}$  is reduced to  $2.6 \times 10^{19} \text{ cm}^{-3}$ , which can be explained by the bandgap renormalization effect. This implies that heavy doping is necessary in high-Al-content AlGa $\text{N}$  alloys to bring down the donor activation energy, therefore a higher conductivity. © 2004 American Institute of Physics. [DOI: 10.1063/1.1825055]

In recent years, Al-rich AlGa $\text{N}$  alloy systems have attracted increasing attention due to their promising material properties that can be used for many optoelectronic applications, such as chip-scale deep UV emitters for chem-bio-threat detection, solid-state lighting for general illumination, solar blind UV photodetectors, and high power/temperature/frequency electronic devices. It is essential to have successful doping and control of conductivity of AlGa $\text{N}$  for these applications. However, it is well known that it is very difficult to achieve highly conductive AlGa $\text{N}$  with high Al content. The difficulty is mainly due to an increase in dislocation density,<sup>1</sup> donor activation energy,<sup>2</sup> and a compensation effect from acceptor-like defects,<sup>3</sup> with increasing Al content. Other possible effects include negatively charged vacancies ( $V_{\text{Ga}}, V_{\text{Al}}$ )<sup>3</sup> and Si DX centers.<sup>4</sup> We have previously reported  $n$ -type conductive  $\text{Al}_x\text{Ga}_{1-x}\text{N}$  alloys for  $x$  up to 0.7; A resistivity value of  $0.15 \Omega \text{ cm}$  with a free electron concentration  $2.1 \times 10^{18} \text{ cm}^{-3}$  and mobility of  $20 \text{ cm}^2/\text{V s}$  was achieved for  $\text{Al}_{0.65}\text{Ga}_{0.35}\text{N}$ .<sup>5,6</sup> Si-doping in  $\text{Al}_x\text{Ga}_{1-x}\text{N}$  ( $x$  up to 1) was attempted and an electron concentration of  $9.5 \times 10^{16} \text{ cm}^{-3}$  in AlN was obtained; however, the conductivity was too low to be measured.<sup>7</sup> Recently, using In-Si co-doping,  $n$ -type  $\text{Al}_{0.65}\text{Ga}_{0.35}\text{N}$  has been achieved with an electron concentration of  $2.5 \times 10^{19} \text{ cm}^{-3}$  and mobility of  $22 \text{ cm}^2/\text{V s}$  corresponding to a resistivity of  $0.011 \Omega \text{ cm}$ .<sup>8</sup> It is expected that heavy doping can enhance the conductivity through (1) the formation of the impurity band or (2) the screening effect due to increased free and bound charges. Both effects can reduce the effective donor activation energy. For GaN, a Si doping level of only  $\sim 10^{18} \text{ cm}^{-3}$  is required for achieving relatively high conductivity; however, the doping level needs to be much higher for high-Al-content AlGa $\text{N}$  alloys due to the deepening of the donor energy level which results from an increased electron effective mass as well as reduced dielectric constant.

In this letter, we report on epitaxial growth and transport studies of highly conductive  $n$ -type Si-doped  $\text{Al}_{0.7}\text{Ga}_{0.3}\text{N}$  epilayers grown on sapphire substrates by metalorganic chemical vapor deposition. A  $0.5 \mu\text{m}$  AlN epilayer was first deposited on (0001) sapphire substrate with a low temperature

buffer, followed by the growth of Si-doped  $\text{Al}_x\text{Ga}_{1-x}\text{N}$  epilayer with a thickness of about  $1 \mu\text{m}$ . The metalorganic sources used were trimethylgallium (TMGa) for Ga and trimethylaluminum (TMAI) for Al. Blue ammonia and silane ( $\text{SiH}_4$ ) were used as nitrogen and silicon sources, respectively. The Si-dopant concentration was intentionally varied by changing the  $\text{SiH}_4$  flow rate from 6 to 16 ml/min, while keeping other conditions the same. The Si dopant concentration was determined by secondary ion mass spectroscopy (SIMS) measurements (performed by Charles Evans & Associates). Variable temperature Hall-effect (standard Van der Pauw) measurement was employed to study the electron transport properties: electron concentration, mobility, and resistivity. X-ray diffraction (XRD) was used to determine the Al content of the epilayer as well as the crystalline quality. Atomic force microscopy was used to probe the surface morphology; no crack was found in any samples studied here. Photoluminescence (PL) was also used to study the optical properties of these samples. The details of most experimental setups can be found elsewhere.<sup>9</sup>

In Fig. 1, we show the Si concentration profile as mea-

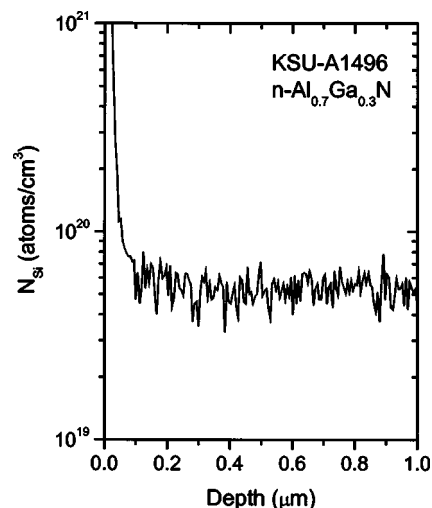


FIG. 1. Silicon dopant concentration ( $N_{\text{Si}}$ ) profiles in an  $\text{Al}_{0.7}\text{Ga}_{0.3}\text{N}$  epilayer with  $\text{SiH}_4$  flow rate of 14 ml/min, as probed by SIMS (performed by Charles Evans & Associate).

<sup>a)</sup>Electronic mail: jiang@phys.ksu.edu

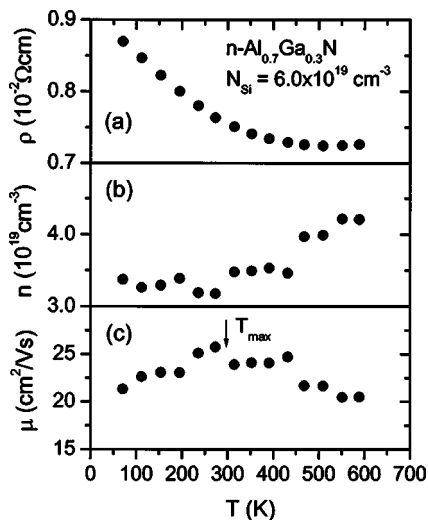


FIG. 2. Variable temperature Hall measurement results of  $n\text{-Al}_{0.7}\text{Ga}_{0.3}\text{N}$  ( $N_{\text{Si}}=6.0 \times 10^{19} \text{ cm}^{-3}$ ). Closed dots are measurement results (from top to the bottom): resistivity  $\rho$ , electron concentration  $n$ , and electron mobility  $\mu$ . In (c),  $T_{\text{max}}$  indicates the characteristic temperature at which electron mobility reaches a maximum value.

sured by SIMS for the sample with  $\text{SiH}_4$  flow rate of 14 ml/min. The result indicates a Si dopant concentration ( $N_{\text{Si}}$ ) of about  $6.0 \times 10^{19} \text{ cm}^{-3}$  in the epilayer. The  $N_{\text{Si}}$  for other samples were calibrated assuming a linear relationship between the measured  $N_{\text{Si}}$  and  $\text{SiH}_4$  gas flow rate.

Figure 2 shows the typical Hall measurement results for the sample with a Si dopant concentration  $N_{\text{Si}}=6.0 \times 10^{19} \text{ cm}^{-3}$  in the temperature range from 70 to 600 K. Resistivity decreases as temperature increases, this is, as expected, due to the fact that more Si impurities are ionized at higher temperatures. This can also be seen from the temperature-dependent electron concentration results, especially in the high temperature range. The electron concentration shows less temperature dependence in the low temperature range, indicating that hopping conduction in the impurity band starts to contribute to the transport process. The mobility initially increases with increasing temperature and reaches a maximum at about 300 K. Similar behavior has been observed and is well understood in GaN: the ionized impurity scattering dominates at low temperature, while polar optical phonon scattering dominates at the high temperature end, which results in a maximum in the electron mobility. For  $n$ -type GaN, this maximum normally appeared around 100 K.<sup>10</sup> However, this maximum shifts to a much higher temperature around 300 K [cf.  $T_{\text{max}}$  in Fig. 2(c)] in 70% Al content AlGa<sub>0.3</sub>N alloys. This shifting is most likely related to the increased ionization energy of Si donors in  $\text{Al}_{0.7}\text{Ga}_{0.3}\text{N}$  compared to GaN, since ionized impurity scattering only becomes important when most donors start to be ionized. We believe that the coincidence of the mobility maximum with room temperature is in fact good for device applications, since most devices will be operated at room temperature.

In Fig. 3, we show the temperature-dependent resistivity results for all samples with varying Si-dopant concentrations from 2.6 to  $6.8 \times 10^{19} \text{ cm}^{-3}$  (as indicated in the figure). The topmost curve is for the sample with the lowest dopant concentration ( $N_{\text{Si}}=2.6 \times 10^{19} \text{ cm}^{-3}$ ), for which we observe a clear thermal activation process. This temperature dependence becomes less evident as the Si-doping level increases,

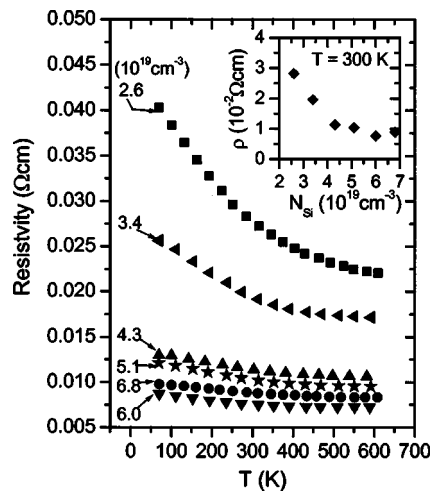


FIG. 3. Temperature-dependent resistivity results for  $n\text{-Al}_{0.7}\text{Ga}_{0.3}\text{N}$  with varying Si doping levels from 2.6 to  $6.8 \times 10^{19} \text{ cm}^{-3}$ . Strong thermal activation process is evident for the sample with the lowest doping level. At high doping levels, samples exhibit degenerated behavior. The inset shows the room temperature resistivity as a function of the Si dopant concentration,  $N_{\text{Si}}$ ; there is a clear trend of decreasing of resistivity with increasing Si doping level. Resistivity as low as  $0.0075 \Omega \text{ cm}$  was achieved for  $n\text{-Al}_{0.7}\text{Ga}_{0.3}\text{N}$  when  $N_{\text{Si}}=6.0 \times 10^{19} \text{ cm}^{-3}$ .

which indicates the trend of moving toward the metallic behavior due to heavy Si doping. The sample reaches its lowest resistivity at  $N_{\text{Si}}=6.0 \times 10^{19} \text{ cm}^{-3}$ . Further increasing of Si-doping level ( $N_{\text{Si}}=6.8 \times 10^{19} \text{ cm}^{-3}$ ) results in an increase in resistivity. This could be due to the self-compensation effect or scattering from heavily doped impurity atoms. This trend is more obvious from the inset of Fig. 3, which shows the doping level dependence of the room temperature resistivity.

The transition toward metallic behavior at high Si doping levels can be understood in terms of Mott transition model.<sup>11</sup> Mott density ( $N_{\text{Mott}}$ ) can be approximately calculated by using  $N_{\text{Mott}} \approx (4.2a_B^3)^{-1}$ , in which  $a_B$  is the donor Bohr radius. Using a linear relation of the parameters between GaN ( $\epsilon=9.5$  and  $m_e^*/m_e=0.2$ ) and AlN ( $\epsilon=8.5$  and  $m_e^*/m_e=0.4$ ), we can obtain  $N_{\text{Mott}}$  of about  $9 \times 10^{19} \text{ cm}^{-3}$  for  $\text{Al}_{0.7}\text{Ga}_{0.3}\text{N}$ . It is, therefore, expected that Si dopants in  $\text{Al}_{0.7}\text{Ga}_{0.3}\text{N}$  start to form an impurity band at a donor concentration close to  $N_{\text{Mott}}$  (for example,  $N_{\text{Si}} \geq 6.0 \times 10^{19} \text{ cm}^{-3}$ , the high limit of the  $N_{\text{Si}}$  in this study, which leads to a metallic behavior of the sample).

The temperature dependence of the resistivity data can be understood with a two-level activation model. At low temperatures, most electrons are localized at the donor impurity sites, which contribute less to the conductivity. As we increase the temperature, more electrons are activated into the conduction band. In the inset of Fig. 4, we show the Arrhenius plot of the electron concentration for the sample with  $N_{\text{Si}}=6.0 \times 10^{19} \text{ cm}^{-3}$ . The solid line is the least-squares fit of data with the charge neutrality equation:

$$\frac{n(n+N_A)}{N_D-N_A-n} = \frac{N_C}{g} \exp\left(-\frac{E_0}{kT}\right), \quad (1)$$

where  $n$ ,  $N_D$ ,  $N_A$  are electron, donor, and acceptor concentrations, respectively.  $N_C$  is the conduction band effective density of states,  $E_0$  is the donor activation energy,  $g$  is the donor degeneracy factor (which is 2), and  $k$  is Boltzmann's constant. Since the impurity-band or hopping conduction con-

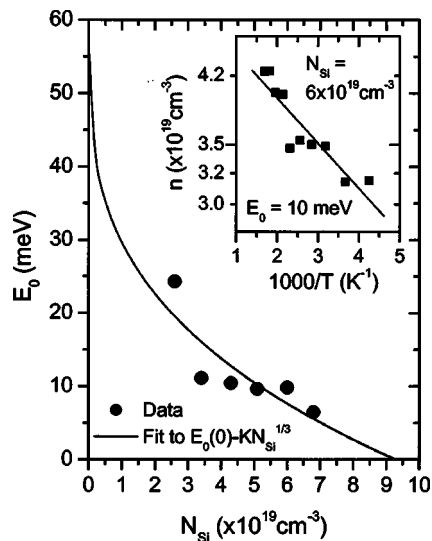


FIG. 4. The Si donor activation energy in  $\text{Al}_{0.7}\text{Ga}_{0.3}\text{N}$  as a function of dopant concentration,  $N_{\text{Si}}$ . Closed dots are measured values and solid line is the least-squares fit with the band gap renormalization effect of Eq. (2). The inset shows the Arrhenius plot of the electron concentration for  $n\text{-Al}_{0.7}\text{Ga}_{0.3}\text{N}$  with  $N_{\text{Si}}=6.0 \times 10^{19} \text{ cm}^{-3}$ ; the solid line is the least-squares fit of data with Eq. (1) with the fitted activation energy of 10 meV.

tribute more to the transport process in the low temperature range, we fitted the data in the high temperature range from 250 to 600 K; a value  $E_0$  of 10 meV was obtained for this sample.

We applied the same fitting procedure for samples with varying dopant concentrations, and the results are presented in Fig. 4. There is a clear trend that  $E_0$  decreases as Si-doping level increases. We attribute this to the band gap renormalization effect due to the screening by free and bound charges,<sup>12,13</sup> and it can be described by

$$E_0 = E_0(0) - K(N_{\text{Si}})^{1/3}, \quad (2)$$

where  $K$  is the renormalization constant,  $E_0(0)$  is the extrapolated activation energy at  $N_{\text{Si}}=0$ . In Fig. 4, the solid line represents the least-squares fit of  $E_0$  with Eq. (2).  $E_0(0)$  was obtained as 55 meV. A simple calculation using effective mass theory shows that the binding energy for a shallow donor in  $\text{Al}_{0.7}\text{Ga}_{0.3}\text{N}$  alloys is about 60 meV using the same parameters we used to estimate  $N_{\text{Mott}}$ , which is consistent with our experimental result.  $K$  was obtained as  $1.2 \times 10^{-5} \text{ meV cm}$ , which is also consistent with a value ( $2.1 \times 10^{-5} \text{ meV cm}$ ) suggested for GaN.<sup>14,15</sup> Our results shown in Fig. 4 suggest that heavy doping is needed to achieve highly conductive  $\text{Al}_x\text{Ga}_{1-x}\text{N}$  alloys with high  $x$  for device applications. Another interesting parameter we could obtain from Eq. (2) is the maximum Si-doping level required to bring  $E_0$  down to zero. Using the fitting results, we extrapo-

late this doping level to be about  $9.5 \times 10^{19} \text{ cm}^{-3}$ , which agrees well with the Mott density. However the resistivity data shown in Fig. 3 from the sample with the highest doping level ( $N_{\text{Si}}=6.8 \times 10^{19} \text{ cm}^{-3}$ ) of the current set is already behaving differently from the expectation. This could be due to the reduction in material quality under extremely high doping level conditions. The XRD and PL results (not shown) for this set of samples also suggest that the sample with the highest doping level has lower crystalline and optical qualities, which is consistent with the Hall results. This implies that there is still room for improvement in material quality and, hence, the conductivity. We also found that the  $T_{\text{max}}$  shifts from 400 to 300 K as the Si doping level is increased from 2.6 to  $6.8 \times 10^{19} \text{ cm}^{-3}$  (not shown), and this is due to the lowering of  $E_0$  as discussed before.

In summary, highly conductive ( $\rho=0.0075 \text{ } \Omega \text{ cm}$ )  $n$ -type  $\text{Al}_{0.7}\text{Ga}_{0.3}\text{N}$  by heavy doping with silicon atoms ( $N_{\text{Si}}=6.0 \times 10^{19} \text{ cm}^{-3}$ ) has been achieved. Silicon was found to act as a shallow donor with an activation energy  $E_0$  ranging from 25 to 7 meV as the silicon doping level was varied from 2.6 to  $6.8 \times 10^{19} \text{ cm}^{-3}$ , which is due to the band gap renormalization effect. We suggest that a minimum silicon doping level of  $10^{19} \text{ cm}^{-3}$  is necessary for achieving high conductivities in AlGa<sub>x</sub>N alloys with high Al contents for device applications.

This research is supported by grants from DOE, NSF, ARO, and DARPA.

- <sup>1</sup>B. Jähnen, M. Albrecht, W. Dorsch, S. Christiansen, H. P. Strunck, D. Hanser, and R. F. Davis, *MRS Internet J. Nitride Semicond. Res.* **3**, 39 (1998).
- <sup>2</sup>A. Y. Polyakov, N. B. Smirnov, A. V. Govorkov, M. G. Milvidskii, J. M. Redwing, M. Shin, M. Skowronski, D. W. Greve, and R. G. Wilson, *Solid-State Electron.* **42**, 627 (1998).
- <sup>3</sup>C. Stampfl and C. G. Van der Walle, *Appl. Phys. Lett.* **72**, 459 (1998).
- <sup>4</sup>S. Fisher, C. Wetzel, E. E. Haller, and B. K. Meyer, *Appl. Phys. Lett.* **67**, 1298 (1995).
- <sup>5</sup>J. Li, K. B. Nam, J. Y. Lin, and H. X. Jiang, *Appl. Phys. Lett.* **79**, 3245 (2001).
- <sup>6</sup>K. B. Nam, J. Li, M. L. Nakarmi, J. Y. Lin, and H. X. Jiang, *Appl. Phys. Lett.* **81**, 1038 (2002).
- <sup>7</sup>Y. Taniyasu, M. Kasu, and N. Kobayasu, *Appl. Phys. Lett.* **81**, 1255 (2002).
- <sup>8</sup>P. Cantu, S. Keller, U. K. Mishra, and S. P. DenBaars, *Appl. Phys. Lett.* **82**, 3683 (2003).
- <sup>9</sup><http://www.phys.ksu.edu/area/GaNgroup>
- <sup>10</sup>A. Saxler, D. C. Look, S. Elhamri, J. Sizelove, W. C. Mitchel, C. M. Sung, S. S. Park, and K. Y. Lee, *Appl. Phys. Lett.* **78**, 1873 (2001).
- <sup>11</sup>N. F. Mott and W. D. Twose, *Adv. Phys.* **10**, 107 (1961).
- <sup>12</sup>H. C. Casey and F. Stern, *J. Appl. Phys.* **47**, 631 (1976).
- <sup>13</sup>K. B. Nam, M. L. Nakarmi, J. Li, J. Y. Lin, and H. X. Jiang, *Appl. Phys. Lett.* **83**, 2787 (2003).
- <sup>14</sup>B. K. Meyer, D. Volm, A. Graber, H. C. Alt, T. Detchprohm, A. Amano, and I. Akasaki, *Solid State Commun.* **95**, 597 (1995).
- <sup>15</sup>D. C. Look and R. J. Molnar, *Appl. Phys. Lett.* **70**, 3377 (1997).